# ORIGINAL RESEARCH

A Novel Humanized Model of NASH and Its Treatment With META4, A Potent Agonist of MET

Jihong Ma,[1,a] Xinping Tan,[1] Yongkook Kwon,[1] Evan R. Delgado,[1,2,3] Arman Zarnegar,[1] Marie C. DeFrances,[1,2,3] Andrew W. Duncan,[1,2,3] and Reza Zarnegar[1,2,3]

[1]The Department of Pathology, University of Pittsburgh, School of Medicine, [2]Pittsburgh Liver Research Center, School of Medicine, and the [3]McGowan Institute of Regenerative Medicine, University of Pittsburgh, Pittsburgh, Pennsylvania.
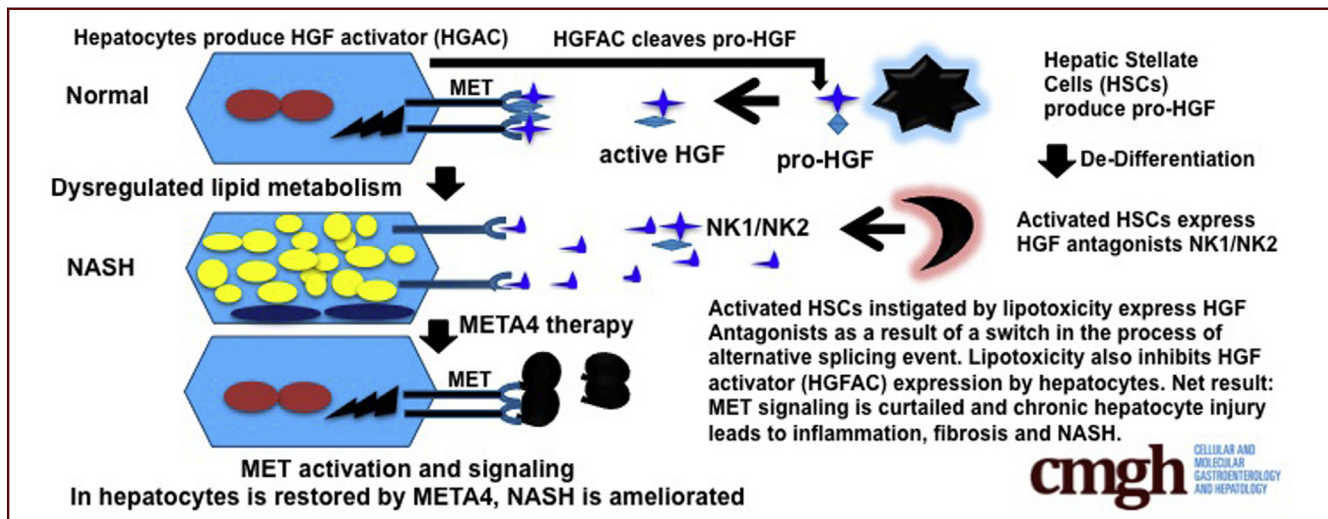
SUMMARY

Our studies reveal that the humanized nonalcoholic steatohepatitis (NASH) model recapitulate human NASH and uncover that hepatocyte growth factor (HGF)-MET function is impaired in this disease. The results show that HGF-MET signaling is compromised in NASH by virtue of upregulation of HGF antagonist and down-regulation of HGF activation. We show that restoring HGF-MET action by META4, an engineered agonist of HGF-MET axis, ameliorates NASH.

BACKGROUND & AIMS: Nonalcoholic fatty liver disease is a frequent cause of hepatic dysfunction and is now a global epidemic. This ailment can progress to an advanced form called nonalcoholic steatohepatitis (NASH) and end-stage liver disease. Currently, the molecular basis of NASH pathogenesis is poorly understood, and no effective therapies exist to treat NASH. These shortcomings are due to the paucity of experimental NASH models directly relevant to humans.

METHODS: We used chimeric mice with humanized liver to investigate nonalcoholic fatty liver disease in a relevant model. We carried out histologic, biochemical, and molecular approaches including RNA-Seq. For comparison, we used side-by-side human NASH samples.

RESULTS: Herein, we describe a "humanized" model of NASH using transplantation of human hepatocytes into fumarylacetoacetate hydrolase-deficient mice. Once fed a high-fat diet, these mice develop NAFLD faithfully, recapitulating human NASH at the histologic, cellular, biochemical, and molecular levels. Our RNA-Seq analyses uncovered that a variety of important signaling pathways that govern liver homeostasis are profoundly deregulated in both humanized and human NASH livers. Notably, we made the novel discovery that hepatocyte growth factor (HGF) function is compromised in human and humanized NASH at several levels including a significant increase in the expression of the HGF antagonists known as NK1/NK2 and marked decrease in HGF activator. Based on these observations, we generated a potent, human-specific, and stable agonist of human MET that we have named META4 (Metaphor) and used it in the humanized NASH model to restore HGF function.

CONCLUSIONS: Our studies revealed that the humanized NASH model recapitulates human NASH and uncovered that HGF-MET function is impaired in this disease. We show that restoring HGF-MET function by META4 therapy ameliorates NASH and reinstates normal liver function in the humanized NASH model. Our results show that the HGF-MET signaling pathway is a dominant regulator of hepatic homeostasis. (Cell Mol Gastroenterol Hepatol 2022;13:565–582; https://doi.org/10.1016/j.jcmgh.2021.10.007)

Nonalcoholic fatty liver disease (NAFLD) has become a global health burden as determined by comprehensive meta-analyses.[1,2] NAFLD is a manifestation of metabolic syndrome, which is highlighted by insulin resistance, obesity, and Type 2 diabetes.[3,4] NAFLD covers a range of pathologies from a benign fatty liver phenotype (steatosis or excessive lipid accumulation in hepatocytes) to a severe form called nonalcoholic steatohepatitis (NASH), which is accompanied by sustained liver inflammation, hepatocyte death, and liver fibrosis. NASH can progress to end-stage liver disease and hepatocellular carcinoma.[5] It is predicted that 20 million NASH-related deaths will occur annually worldwide, surpassing hepatitis C and hepatitis B virus-related liver mortality.[2] Cirrhosis due to NASH is anticipated to become the most common indication for liver transplantation. No effective drugs currently exist to treat NASH.[4,5] This is due to lack of models of NASH that are directly relevant to humans, as most of the present models rely on rodents (mainly mouse and rat). It is well-known that significant differences exist between human and rodent hepatocytes,[6,7] especially with regard to the metabolic pathways that go awry in NAFLD, particularly those of lipid and carbohydrate metabolism. The development of a model that closely recapitulates human liver will not only facilitate a better understanding of the molecular mechanisms involved in NAFLD pathogenesis and progression but will also provide a platform for rational drug design and testing. Herein, we describe a novel "humanized" model of NASH and show that the humanized liver develops all the hallmarks of human NASH, mirroring the human disease counterpart at the histologic, cellular, biochemical, and molecular levels. Our molecular analyses using RNA-Seq, microarray, and proteomic analyses uncovered that a variety of important signaling pathways that govern hepatic homeostasis are profoundly deregulated in humanized and human NASH livers. The impacted biological processes include pathways regulating glucose and fat metabolism, inflammation, oxidative stress, hepatocyte death, and hepatocyte proliferation, to name a few. Notably, we discovered that hepatocyte growth factor (HGF) action is blocked in NASH at several steps including upregulation of HGF antagonists called NK1 and NK2 and decrease level of HGF activator (HGFAC). Based on these observations showing that HGF is rendered nonfunctional in NASH, we generated a potent specific and stable agonist of human MET (the receptor for HGF) that we have named META4 and used it to reconstitute HGF function and treat NASH in the humanized model. Our novel study reveals that META4 therapy can efficiently ameliorate NASH and restore normal liver function.

Results

Humanized Livers Develop Nonalcoholic Fatty Liver Disease

To generate a humanized NAFLD model, we took advantage of mice deficient in fumarylacetoacetate hydrolase (FAH), an enzyme responsible for catabolism of tyrosine known as FRGN, the livers of which can be repopulated with human hepatocytes.[8,9] This humanized chimeric mouse model has been proposed to be an invaluable tool to study drug metabolism, excretion, and toxicity in a system more relevant to humans.[10,11] In our studies, we used the humanized mice approximately 6 months after they were subjected to the transplantation protocol. We tested whether the transplanted mice (henceforth referred to as humanized mice) develop a fatty liver phenotype if fed a high-fat diet (HFD). Accordingly, these mice were randomly divided into HFD and regular diet (RD) groups. Nontransplanted FRGN mice were also used as an additional control cohort. Mice were then fed regular chow (RD) or Harlan Teklad TD.88137 "Western Diet" chow (HFD) for 6 weeks. During the experiment, mice were monitored for food intake and body weight. At the end of 6 weeks, they were culled, and their sera and livers were harvested for histologic, biochemical, and molecular studies. We found that the humanized livers became severely steatotic showing macrovesicular hepatocytic fatty change only if humanized mice were fed an HFD (Figure 1A). Liver and serum triglycerides and cholesterol were also elevated in the humanized mice on HFD (Figure 1B). To show that the transplanted human hepatocytes in fact accumulate fat, we performed immunohistostating for FAH, and the data revealed that the human hepatocytes become steatotic and that host mouse hepatocytes (which are deficient in FAH) exhibit little or no steatosis (Figure 1C, D). Nontransplanted FRGN mice also had little or no steatosis on a HFD for 6 weeks. It should be noted that neither of the human hepatocyte donors had fatty liver at the time of harvest. Mice in general develop NAFLD only after prolonged feeding of a HFD depending on the genetic background (more than 15 weeks).[12] The fat laden human hepatocytes succumbed to lipotoxicity as evidenced by marked inflammatory cell accumulation surrounding the FAH-positive hepatocytes inducing their death as evaluated by TUNEL (Figure 1D, E). The results described in Figure 1 were repeated in a separate set of experiments using FRGN mice transplanted with human hepatocytes from a different donor.

Humanized Liver Recapitulates Human Nonalcoholic Steatohepatitis

A prominent feature of NASH is liver fibrosis, which develops in the background of inflammatory cell infiltration

Figure 1. Mice with humanized liver develop NAFLD if placed on an HFD. *A*, Images of liver sections from humanized liver stained with hematoxylin and eosin (H&E), Oil-Red-O, FAH, and TUNEL as indicated. *Arrows* points to fat-laden hepatocytes. *B*, Liver and serum triglyceride level. N = 4–6 mice per group. Bar graphs depict the relative expression. ***P = .001 and **P = .01, respectively. *C and D*, FAH immunostain. FAH-positive human hepatocytes are marked by *filled arrows* and FAH-negative mouse hepatocytes are marked by *unfilled arrows*. In *D*, note the foci of inflammatory cells surrounding the human hepatocytes. *E*, TUNEL stain. *Arrow* points to the same region positive for FAH. Scale: 100 mm in panels *A*, *C*, *E* and 30 mm in panels *B* and *D*, respectively.


of the hepatic parenchyma. Thus, we compared the humanized liver (Figure 2A) with human liver with clinically proven NASH side-by-side (Figure 2B). We observed infiltration of inflammatory leukocytes, in particular macrophages and neutrophils, ballooning hepatocytes, stellate cell activation, and collagen deposition (Figure 2A, C) in the livers of humanized mice exposed to a HFD akin to human NASH livers. Neither inflammatory cell infiltrate nor liver damage was detected in the humanized mice fed a RD or in the nontransplanted mice placed on a HFD (Figure 2A). The data summarized in Figures 2 and 3 overall show that the humanized mice fed a HFD develop a NASH phenotype like that seen in human NASH at the histologic, cellular, and biochemical levels.

We next carried out whole transcriptome analyses using RNA-Seq and, as a complementary approach, human-specific GeneChip microarray (human Affymetrix U133 Plus 2.0 Array, which has more than 54,000 probes encompassing the whole human encoding transcriptosome) to investigate whether the model genocopies human NASH. In parallel for comparison, we included human normal and NASH livers in our experiments. To avoid bias in data interpretation, samples were anonymized prior to analyses. RNA-seq reads were aligned to the human genome reference to assess the human-specific gene expression profile. The results showed that, in human NASH liver as compared with human normal

liver, the expression of approximately 1280 genes were significantly upregulated, and 600 genes were downregulated ($P < .05$ and at least 1.5-fold changes). About 10,900 genes remained unchanged. When humanized NASH livers were compared with humanized normal livers, close to 1800 genes were significantly induced, 923 genes were repressed, and 8650 genes remained unchanged. We also compared humanized NASH livers with normal human livers and found that the expression of 1180 genes was induced, 1150 genes repressed, and 10,100 genes remained unaffected. In concordance with these data, microarray results revealed the expression of about 1000 genes were upregulated and 600 genes were down-regulated in both human and humanized NASH livers compared with their normal counterpart. Comparison of the groups using bioinformatic tools including Gene Ontology, Kyoto Encyclopedia of Genes and Genomes, and Gene Set Enrichment Analysis analyses revealed that the human and humanized NASH shared similarity in the most highly deregulated biological processes. The common down-regulated processes included: drug metabolism – cytochrome P450, metabolism of xenobiotics by cytochrome P450, and lipid and glutathione metabolism, to name a few and the upregulated processes were inflammatory response, NAFLD pathway, viral infection (ie, hepatitis C and B), degenerative diseases (like Alzheimer and Parkinson diseases), oxidative
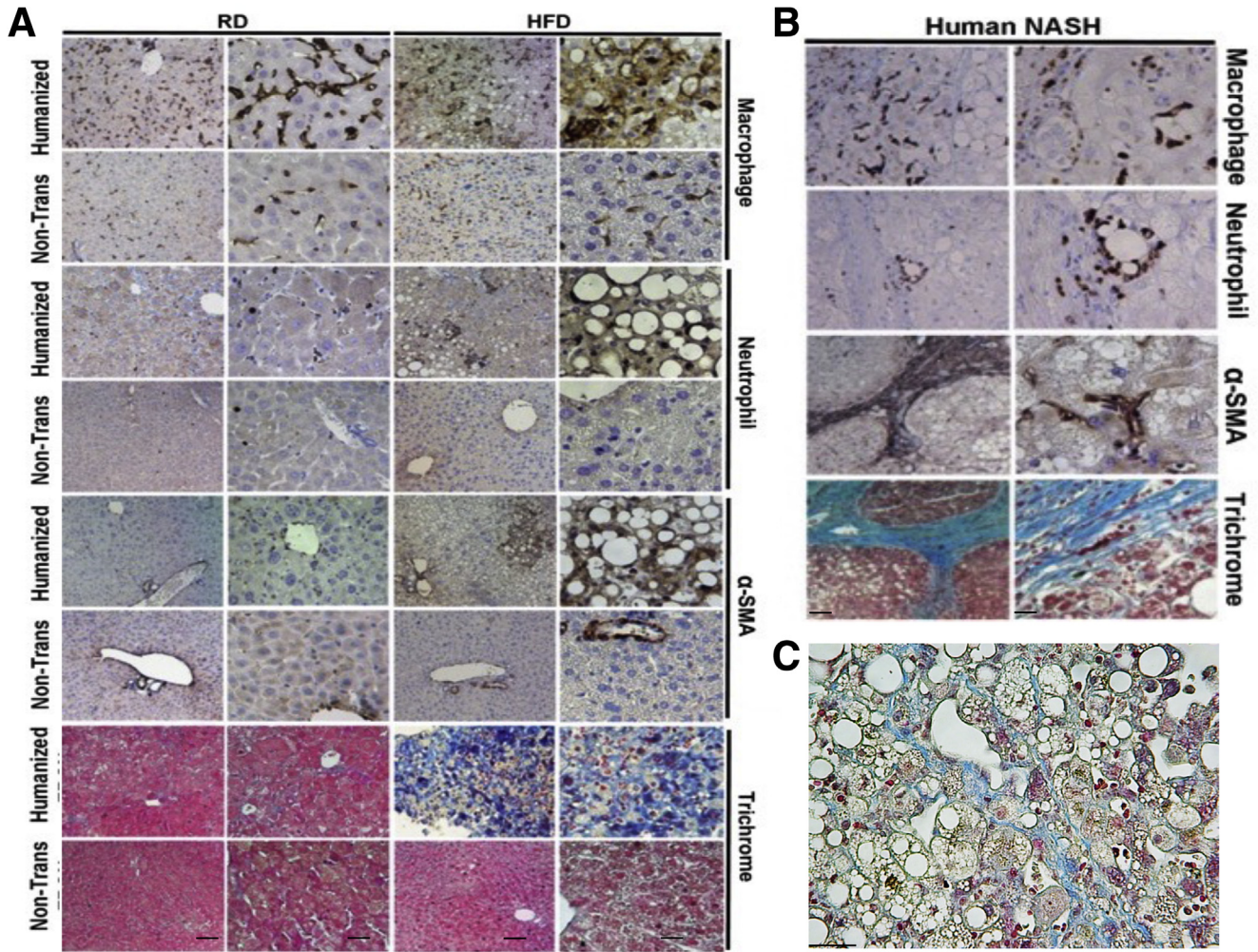
Figure 2. Humanized fatty liver phenocopies human NASH at the histologic, cellular, and biochemical levels. Results shown are from analyses performed side-by-side on the humanized (*A*) and human NASH livers (*B*), and nontransplanted livers for the indicated markers as determined by immunohistochemistry. Scale: 100 mm for *left* and 30 mm for *right* images in each column. *C*, Depicts higher magnification image of humanized liver stained with trichrome for collagen.

phosphorylation, and cell death pathways (such as necroptosis, apoptosis, and ferroptosis) (Figures 4–6). We performed principal component analysis and found that NASH livers co-cluster, and normal livers aggregate together (Figure 7). For a comprehensive list of genes and pathways affected see the Supplementary Table.

We next tested the hypothesis that hepatocyte lipotoxicity generates cues that recruit innate immune inflammatory cells such as macrophages and neutrophils to the liver and induce their expansion promoting liver injury. Accordingly, we aligned the RNA-Seq data from humanized livers to the mouse genomic reference to gain insight into the modification of mouse-specific gene expression in the model. The results uncovered that cytokine and chemokine signaling pathways that activate macrophages and neutrophils and promote leukocyte transendothelial migration are significantly upregulated in humanized NASH liver as compared with humanized normal liver.

Expression of Hepatocyte Growth Factor Antagonist is Upregulated in Nonalcoholic Steatohepatitis

Alternative splicing of a given pre-mRNA transcript can generate mRNA variants yielding protein isoforms with distinct functions. This mode of mRNA generation plays a critical role in homeostasis and disease, and almost one-half of human genes are believed to undergo alternative splicing events.[13] RNA-Seq and microarray mRNA expression profiling are reported to be powerful techniques to detect differentially expressed alternative splice variants. Our RNA-Seq analysis revealed that significant changes in splicing events happen in NASH livers as compared with the corresponding normal livers. We found that in human NASH versus human normal liver, 1647 splice variants of various transcripts were down-regulated and 2433 were upregulated. Similarly, in humanized NASH as compared with the humanized control counterpart, we uncovered that splice

Figure 3. Quantification of the results shown in Figure 2. Graphs in (*A*) and (*B*) depict indicated markers shown in Figure 2 as determined by image analysis. C, Illustrates quantification of collagen content in the liver by measuring hydroxyproline a component of collagen. Nontransplanted FRGN and wild type CD1 mice are also included for comparison. *Asterisks* denote *P* < .05. See text for details.
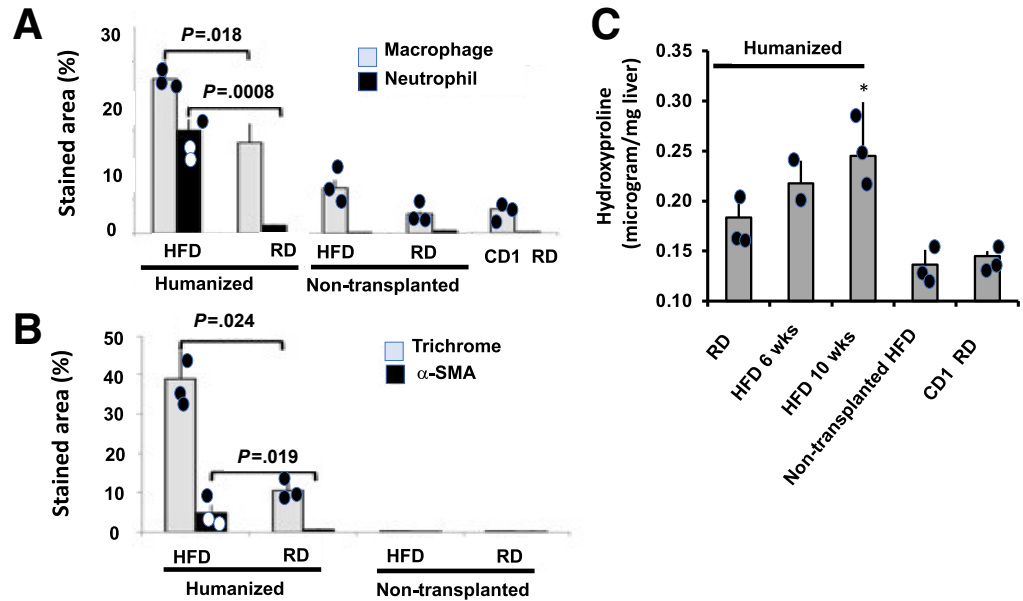
variants of 926 transcripts were upregulated and 869 were down-regulated. Most of the alternative splicing events were of skipped exon type as compared with other classes such as alternative 5′ splice site, alternative 3′ splice site, retained intron, and mutually excluded exons (Figure 8*A*). These transcripts belong to a wide array of biological functions, such as growth and development, autophagy, and metabolism. Some representatives splice variants included: YAP1, FGFR3, BMP1, MAPK5, ATG13, Caspase 8, GSTM4, and SLC22A25 (a solute carrier), which underwent differential alternative splicing events in human and humanized NASH. Consistent with these observations, pathway analyses revealed that significant changes occur in the expression of the components of spliceosome machinery in human and humanized NASH (Figure 8*B*). Importantly, we made the novel observation that the expression of the alternative splice variant of HGF, which generates HGF antagonists called NK1 and NK2, is significantly upregulated in human NASH liver. These isoforms only encode the N-terminal portion of HGF and lack kringles 3 and 4 as well as the entire beta chain of HGF. The NK1 isoform cDNA was first cloned from a human fibroblast cell line,[14] and NK2 was cloned from human placenta.[15] Structure-function studies have shown that the N-terminal region of HGF alpha chain is necessary and sufficient for binding to the HGF receptor (MET) but is unable to activate MET and that the beta chain which is in the C-terminal portion of HGF is required for receptor dimerization and activation.[16] Our RNA-Seq and microarray data revealed that the mRNAs for the HGF antagonists NK1 and NK2 are expressed in normal human liver at low levels but are significantly upregulated in human NASH. To confirm this novel finding, we made reverse primers specific to the 3′-untranslated regions of human NK1 or NK2 and forward primers corresponding to human HGF's N-terminal region. We subsequently performed reverse transcription polymerase chain reaction (PCR) on

human normal and NASH liver, cloned the resulting cDNA and sequenced it. The results proved that NK1 and NK2 mRNAs are indeed expressed in human liver and are highly upregulated in human NASH liver (Figure 9*A*). To extend this finding, we performed Western blot analyses using antibodies specific to the N-terminal region of HGF (which is present in NK1 and NK2). NK1 and NK2 proteins have a predicted Mr of about 25 to 32 kDa, whereas canonical HGF has an Mr of about 70 to 90 kDa (proteolytically cleaved or unprocessed HGF, respectively). Using Western blot analysis, we confirmed that NK1/NK2 proteins are significantly upregulated in human NASH liver and the plasma of patients with NASH (Figure 9*B* and 10, respectively). HGF protein is produced and secreted as a single chain pro-HGF molecule. This precursor is biologically inactive and requires enzymatic cleavage by a specific serine protease called HGFAC, which is expressed by hepatocytes. Notably, our transcriptome and protein analyses revealed that HGFAC mRNA and protein abundance are significantly reduced in human NASH liver as compared with human normal liver (Figure 9*C, D*). Another serine protease system, uPA (urokinase type plasminogen activator) and tPA (tissue type plasminogen activator), has also been shown to cleave pro-HGF to its active double chain form.[17] Interestingly, our transcriptome analyses revealed that the expression of the gene *Serpine1* encoding plasminogen activator inhibitor-1 (PAI-1), a potent inhibitor of uPA and tPA, is significantly induced (by more than 4-fold) in human and humanized NASH liver. Others have also reported that PAI-1 is upregulated in human nonalcoholic and alcoholic fatty liver disease and that PAI-1 is an independent marker of poor prognosis in patients with NAFLD.[18–20]

We next asked if HFD causes a change in hepatic HGF expression in wild type mice (C57BL/6). We discovered that HGF expression is reduced (Figure 11*A*), whereas HGF antagonist NK1 is induced by HFD (Figure 11*B*). To our
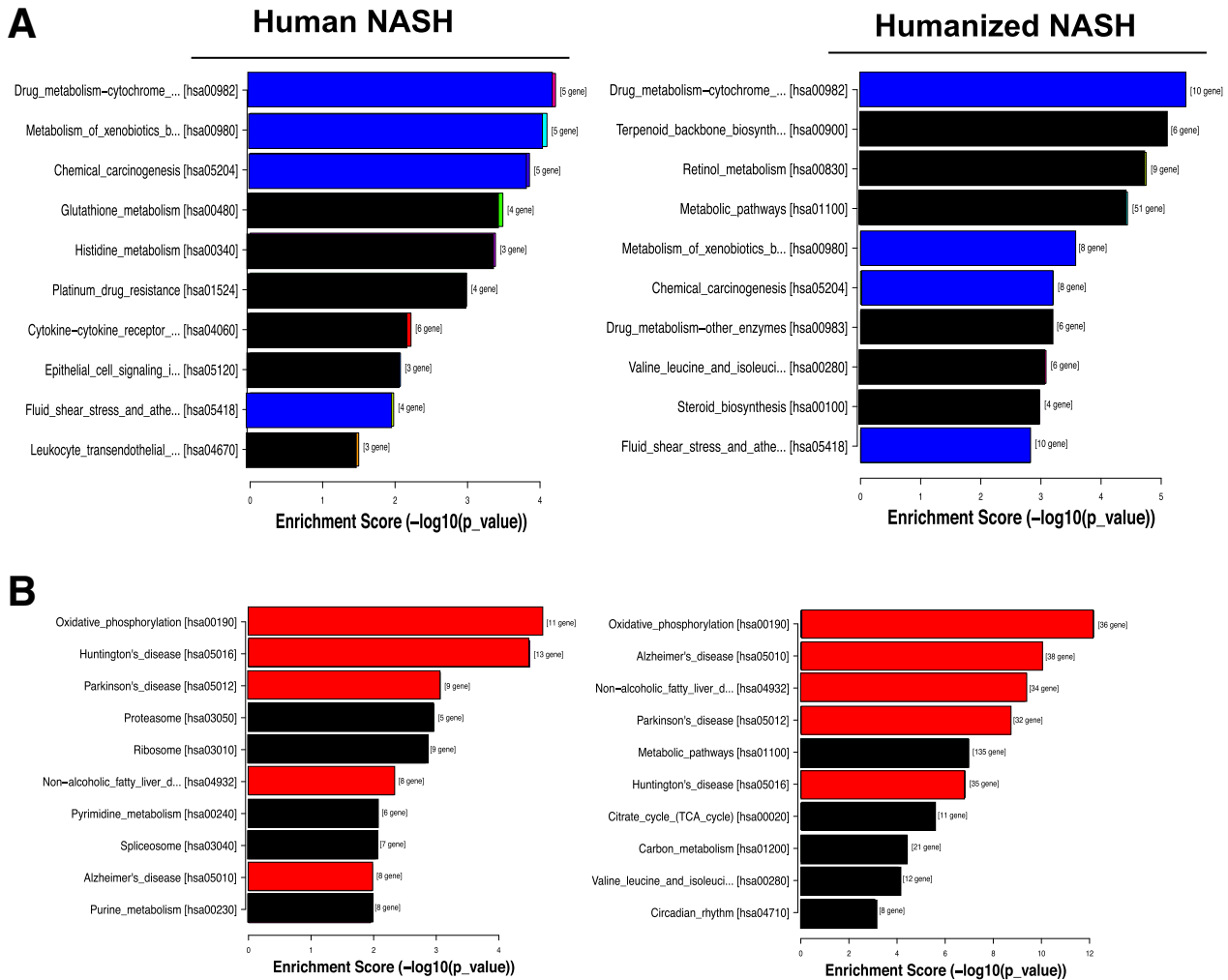
Figure 4. Humanized NASH recapitulates human NASH as determined by RNA-Seq analyses. Shown are examples of the top 10 pathways that are significantly down-regulated (*A*) or upregulated (*B*) in human and humanized NASH livers as compared with their corresponding normal livers. Pathway names and number of genes impacted are indicated in the graphs. Pathways are ordered from top to bottom by *P* values. Bars with *blue* and *red* colors denote identical pathways that are affected in both human and humanized NASH.
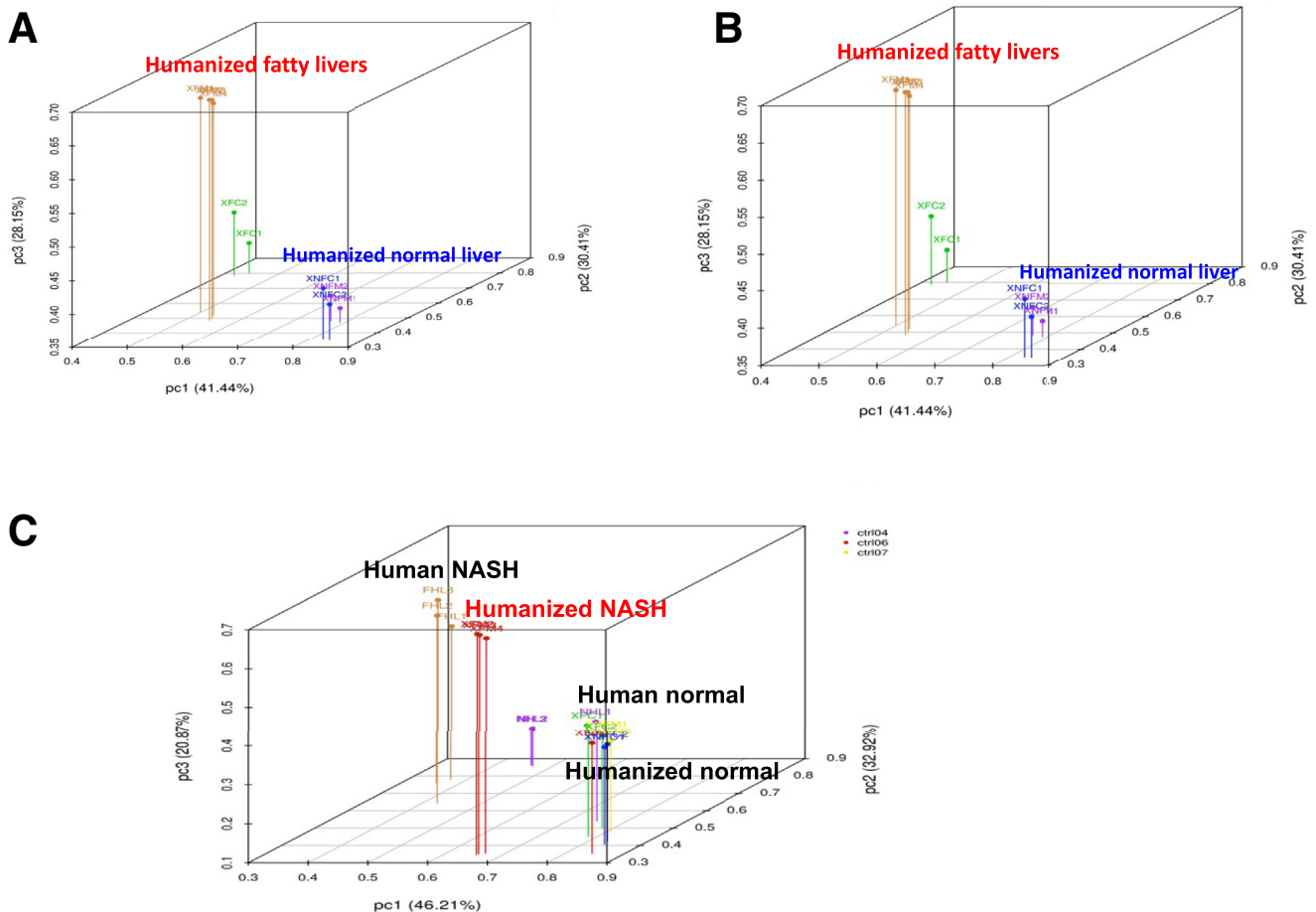
knowledge, this is the first time that the HGF antagonists have been detected in the liver and, more importantly, the first time they are implicated in human disease like NASH. Collectively, our data reveal that HGF function is impaired in NASH liver at several levels via (1) increased expression of HGF antagonists and (2) blockage of pro-HGF activation via reduction in HGFAC and upregulation of PAI-1.

Generation of META4, a Potent Agonist of MET, the Receptor for HGF

The HGF-MET axis governs key aspects of liver homeostasis by promoting the survival and proliferation of hepatocytes as well as liver regeneration.[21–23] Moreover, we have shown that this ligand-receptor system is essential for hepatic glucose and fat metabolism in cooperation with insulin receptor signaling.[24] We reported that systemic injection of HGF into diabetic insulin resistance ob/ob mice restores insulin sensitivity.[24] All of the biological responses of HGF are elicited by its ability to bind to and activate MET, a transmembrane tyrosine kinase receptor.[21,22] Several preclinical studies have suggested that HGF has therapeutic potential as a promoter of tissue regeneration and restoration of homeostasis of various organs including the liver.[25–30] However, the clinical application of HGF has been hampered due to the fact that it binds avidly to heparin and heparan sulfate in the extracellular matrix and, because of this, HGF exhibits poor tissue distribution when injected intravenously, intraperitoneally, subcutaneously, or intramuscularly. HGF administered systemically is also unstable because it is rapidly cleared by the liver and does not reach other organs.[31] Furthermore, as mentioned earlier, HGF is produced as an inactive pro-HGF precursor and requires protease cleavage to become bioactive: disruption of HGF activation renders it ineffective. In fact, in patients with fulminant hepatic failure and in patients with cirrhotic liver,

Figure 5. Pathway of cell death is upregulated in human and humanized NASH. Shown are heat maps of Pathway of Necroptosis [KEGG hsa04217]. *Red* and *blue* colors indicate up- or down-regulated expression, respectively.

plasma pro-HGF is elevated but it is not cleaved, and hence is inactive.[32,33] These findings combined with our data that HGF action is compromised in NASH liver at multiple levels prompted us to therapeutically target the HGF-MET axis in NASH using the humanized NASH model we described herein. We reasoned that generation of an HGF-MET agonist with good pharmacokinetics and stability should overcome HGF's blockage opening avenues for its therapeutic application for organ dysfunction including liver diseases such as NASH.

Monoclonal antibodies that bind to and activate specific growth factor receptors have recently been reported to be

Figure 6. Pathways of viral infection is regulated in human and humanized NASH. Shown are the heatmaps of the hepatitis C [KEGG hsa05160]. *Red* and *blue* colors indicate up- or down-regulated expression, respectively.
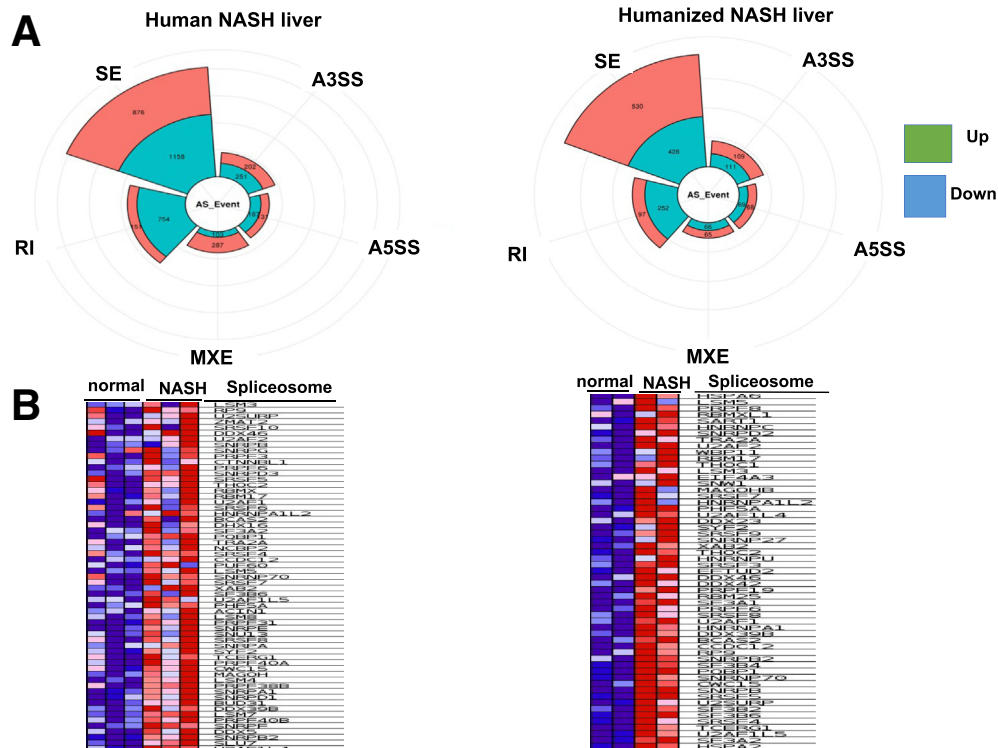
Figure 7. Human NASH and humanized NASH co-cluster as determined by RNA-Seq and principal component analysis (PCA). Shown is the PCA graph. PCA was performed with genes that have the analysis of variance *P* value of .05 or less on FPKM abundance estimations. The Figure is an overview of samples clustering. The result from PCA shows a distinguishable gene expression profiling among the samples. *A*, Normal human liver samples (labeled NHL) co-cluster with each other and human liver samples with NASH (labeled FHL) co-cluster with each other; n = 3 for human non-fatty; n = 3 for human NASH. *B*, Similarly, humanized NASH co-cluster with each other and humanized normal co-cluster together; n = 6 per group. *C*, Human and humanized NASH co-cluster with each other, and human normal and humanized normal group together; n = 3–6 per group.

an effective way to modulate a given receptor in vitro and in vivo. Moreover, antibodies have good tissue distribution and more importantly long plasma half-life (more than 30 days for IgG1). For instance, monoclonal antibody to fibroblast growth factor receptor 1 (FGFR1) was shown to mimic FGF21, activate FGFR1 in adipocytes, and ameliorate hyperglycemia in a mouse model of diabetes.[34,35] Therefore, we generated mouse monoclonal antibodies against the extracellular domain of human MET and screened these antibodies for their ability to activate MET using cell-based assays. Akin to HGF, one clone, which we named META4 (pronounced metaphor), potently and rapidly (within minutes) activated MET and its downstream effectors, such as Gab-1 (an IRS family member), Akt, and Erk in human hepatocytic cell lines like HepG2 hepatocytes (Figure 12*A*). Given, the fact that META4 was raised against human MET extracellular domain (also called the ectodomain), we wanted to explore if META4 activated rodent MET. We found that META4 is highly specific for human MET and does not stimulate mouse MET using mouse hepatocytes cultures (Figure 12*B*). This finding led us to hypothesize that the epitope-binding site of META4 on human MET is not conserved in rodent MET. Sequence alignment analyses revealed that the amino acid sequence of the extracellular domain of MET is not fully conserved between human and rodents, but it is highly conserved between human and nonhuman primates like rhesus monkeys. We next tested if META4 activates MET in cells derived from nonhuman primates. We stimulated the normal kidney epithelial cell line LLC-MK2 from rhesus monkey with META4 and discovered that META4 efficiently activates MET in these cells like human kidney epithelial HEK-293 cell line (Figure 12*C*). We cloned the META4 cDNAs (ie, light and heavy chains) from META4-producing hybridoma cells and expressed the cloned cDNAs in HEK293 cells, purified the recombinant META4 by protein-A chromatography and

Figure 8. Pronounced changes in mRNA alternative splicing events occur in human NASH and humanized NASH livers as determined by RNA-Seq and pathway analyses. Humanized and human NASH liver was analyzed side-by-side using RNA-Seq and gene set enrichment analysis (GSEA). *A*, Depicted is the differential alternative splicing (AS) events summary plots for human and NASH livers as compared with their corresponding normal livers. Upregulated transcript variants are shown in *red* and downregulated in *green* colors, respectively. Splice types are: skipped exon (SE), alternative 5′ splice site (A5SS), alternative 3′ splice site (A3′SS), retain intron (RI), and mutually excluded (MXE) exons. Numbers in the plot correspond to transcript numbers involved. *B*, Heat maps of the spliceosome pathway (KEGG-HSA03040) impacted in human and humanized NASH livers. Upregulated transcript variants are shown in *red* and down-regulated in *blue* colors, respectively; n = 6 for human and n = 4 for humanized livers.

evaluated it for its ability to activate MET. Figure 12D illustrates that purified recombinant META4 is a strong activator of MET in human hepatocytes. Finally, we tested whether META4 activates MET signaling in humanized mice. The results showed that indeed META4 potently induces MET and its down-stream effectors like IRS and glycogen synthase in the livers of humanized mice (Figure 13).

META4 Therapy Ameliorates Nonalcoholic Steatohepatitis in a Humanized Model of Nonalcoholic Fatty Liver Disease

Given the above results showing that HGF-MET axis is compromised in NASH and that META4 protected hepatocytes against lipotoxicity by promoting hepatocyte homeostasis (by impacting metabolic processes as well as fostering hepatocyte survival and regeneration), we were prompted to test if META4 has therapeutic potential against NASH using the humanized model that we described above. Accordingly, we divided a cohort of humanized mice into experimental (injected with META4) and control (injected with isotype-matched mouse IgG1) groups (n = 7 per group). These mice were placed on HFD and then treated with META4 or isotype matched mIgG1 (control-treated).

META4 therapy was administered for 4 weeks. During these experiments, we monitored the mice for food intake and body weight. At the end of the experiment, we collected their sera and livers for histologic, biochemical, and molecular studies as described for Figure 2. The results demonstrated that control (mIgG1) treated mice exhibited marked pericellular fibrosis, which was accompanied by pronounced macrophage and neutrophil infiltration. Notably, META4 treatment inhibited inflammatory cell infiltration, ameliorated fibrosis, halted hepatocyte death, and stimulated marked proliferation of human hepatocytes (co-staining with Ki-67 and FAH) (Figures 14 and 15).
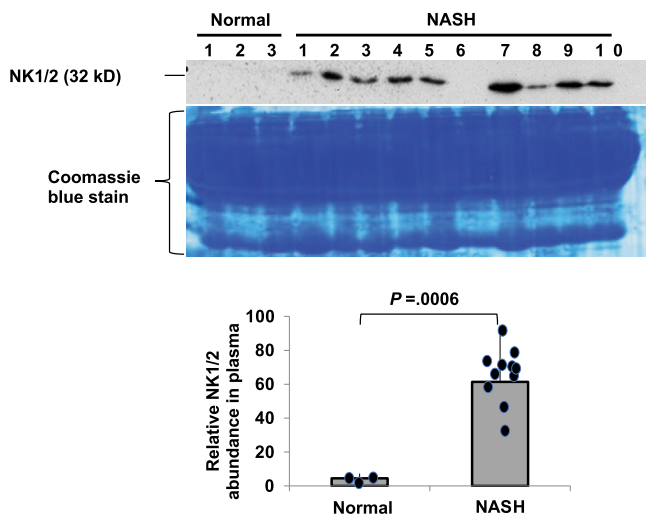
It is well-known that when the protective drug NTCB is withdrawn from FRGN mice and if they are not transplanted with FAH-proficient hepatocytes or the proliferation and survival of the transplanted hepatocytes is inhibited (in our case, due to lipotoxicity), the animals lose weight, become sick by 4 weeks, and die due to massive host hepatocyte death, liver failure, and its associated secondary pathologies. Therefore, to decipher the pro-growth, pro-regenerative activities of META4 on the homeostasis of the transplanted hepatocytes under the lipotoxic conditions, mice were subjected NTBC regimen consisting of 3 cycles of NTBC withdrawal lasting 2 weeks for each cycle. We found that the

Figure 9. HGF antagonists NK1 and NK2 are expressed in human NASH liver. *A*, Results of RT-PCR (n = 3 cases per group); and *B*, Western immunoblot for HGF antagonist (n = 5 cases per group) using antibody to the N-terminal region of HGF. Bar graphs depict the relative expression. *C*, *D*, HGFAC expression is significantly reduced in the livers of humans with NASH. *C*, Shown is the relative abundance of HGF activator transcript in human liver as determined by RNA-seq. *P = .02. *D*, Depicted are the Western blot results for HGFAC in human normal and NASH livers (n = 5 and n = 6 cases per group as indicated).
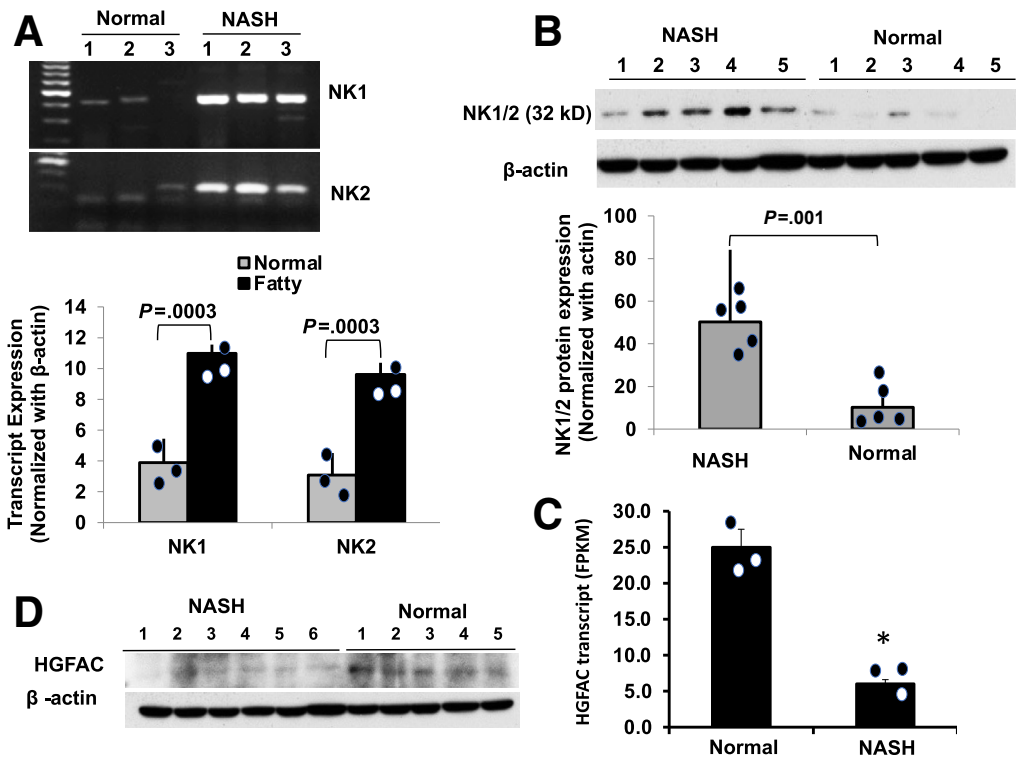
control (mIgG1) treated mice gradually lost weight and became moribund leading to the control mice dying by 4 weeks, whereas META4-treated mice survived, behaved normally, and did not lose weight (Figure 16A). It should be

Figure 10. HGF antagonist is present in the plasma of patients with NASH. Shown are the results of Western immunoblot of plasma samples (3 microliters) using antibody to the N-terminal region of HGF. Coomassie blue stain of the gel is shown below the blots. Coomasie blue stain of gel is shown for equal loading of plasma samples. Bar graphs depicts the relative expression of NK1/NK2 signals. NASH (n = 10 different cases) and normal (n = 3 different cases).

noted that no major inflammatory cell infiltrate and no liver damage were detected in humanized mice on RD or in the non-transplanted mice placed on HFD or on RD with the same NTBC regimen we used for the humanized mice (see Figure 2). One of the clinical hallmarks of NAFLD is hepatomegaly. Of note, we found that META4 therapy dampened this feature in humanized NASH. Specifically, the liver to body ratio in control-treated mice was 15%, and it was reduced significantly (P = .01) in META4-treated mice by 4 weeks of therapy (Figure 16B).

META4 Therapy Corrects the Expression of Key Hepatic Genes That are Deregulated in NASH

To gain further insight into the molecular mechanisms by which the HGF-MET signaling axis in the liver maintains hepatic homeostasis (and ameliorates NASH), we carried out RNA-Seq on livers from humanized mice that were treated with META4 or control mIgG1. The results provided a wealth of information revealing that the HGF-MET signaling axis in the liver governs key pathways that regulate hepatic homeostasis. In brief, RNA-Seq results revealed that the expression of approximately 1800 genes was significantly changed by META4 treatment as compared with the control treatment (mIgG1). About 1112 genes were down regulated, 750 genes were induced, and 9300 genes remained unaffected. Bioinformatic analysis uncovered that the affected genes belong to various pathways such as metabolism, growth, cell survival, and cell death. Specifically, the MET signaling axis suppressed the pathways of NAFLD,

A

B
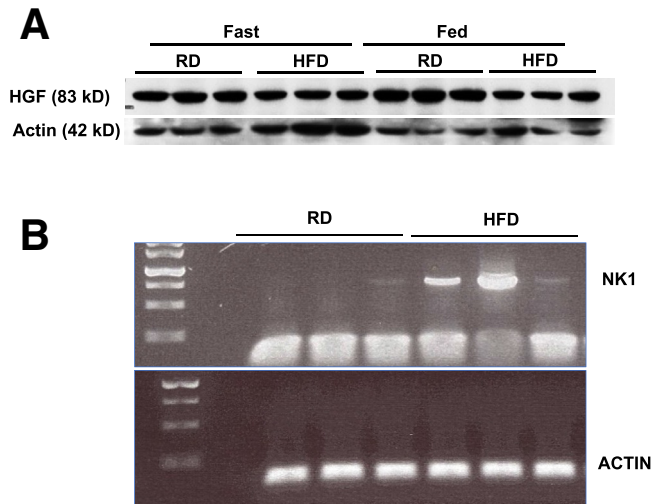
Figure 11. **HGF expression is reduced in the liver of wild-type mice C57/Bl6 fed a HFD whereas that of HGF antagonist is induced.** *A*, Western blot data for HGF; and *B*, RT-PCR results for NK1 expression. Animals were culled at feed or after an overnight fast as indicated. Mice were fed on HFD for 3 months.

oxidative stress, inflammation, cell death, NFkB, chemokine, and tumor necrosis factor-alpha (Figure 17*A, B*). Pathways that were upregulated by META4 encompass those that are involved in glucose and fat metabolism, drug metabolism, insulin signaling, bile secretion, and antioxidation (Figure 17*C*). Examples of genes upregulated by META4 include CYP3A4, CYP2E1, and CYP3A7 (which are the key regulators of bile acid synthesis and xenobiotic metabolism), and antioxidant enzymes like catalase and glutathione S-transferase. For a comprehensive list of genes and pathways impacted by META4, see the Supplementary Table.

Discussion

The studies presented in this paper have several salient features. First, we developed a humanized model of NASH that recapitulates its human disease counterpart. Second, we made the major discovery that the HGF-MET system is compromised (blocked) in human NASH at various levels including upregulation of HGF antagonists NK1 and NK2, down-regulation of HGF activator enzyme called HGFAC, and upregulation of PAI1, a potent inhibitor of uPA/tPA, enzymes that can activate HGF. To our knowledge, our
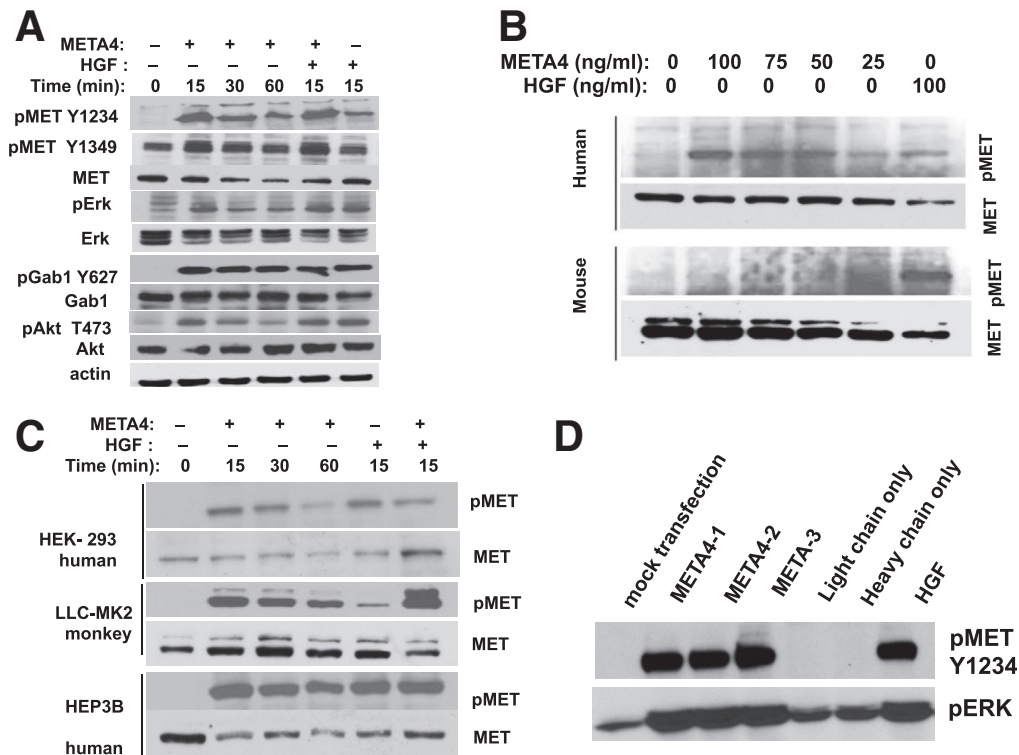
Figure 12. **Robust and rapid activation of MET and MET signaling effectors by META4.** A, Activation of MET in human hepatocyte cell line HepG2; shown is the Western blot for the indicated effectors. *B*, META4 does not activate rodent MET. Western blot data showing that META4 activates MET in human but not mouse hepatocytes (Hepa 1-6 cell line). Cells were treated for 15 minutes and processed for MET activation (pMET 1234Y) and total MET as indicated. HGF was used as a positive control, which activates mouse and human hepatocytes. *C*, META4 activates MET in non-human primates Rhesus monkey kidney epithelial cell line LLC-MK2 and in human kidney epithelial cell line HEK-293. *D*, Production of active re-combinant META4. HEK-293 ells were transfected with META4 heavy plus light chain expression vectors or by individual chains as indicated. Culture media were harvested 5 days post-transfection, and META4 was purified by protein-A chro-matography. Activity was assessed by MET activation as in (*A*).
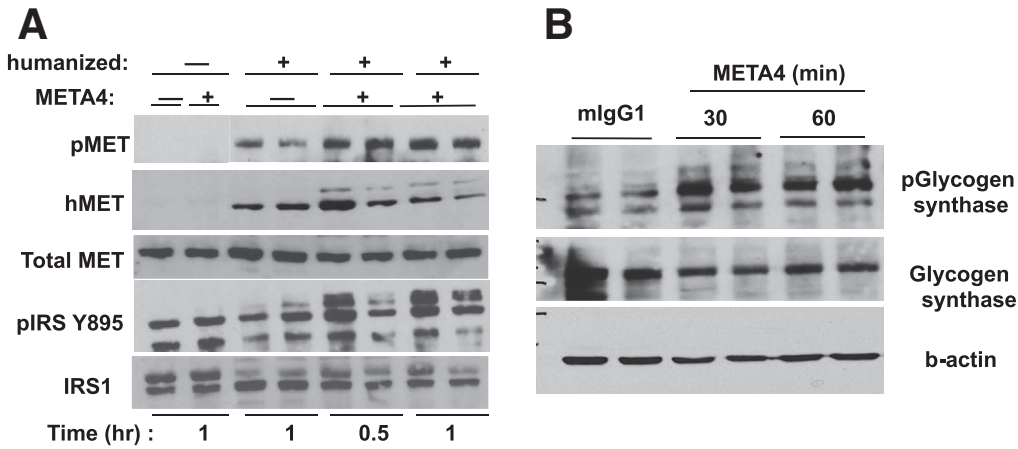
Figure 13. META4 activates MET and MET in humanized mice liver. META4 was injected intraperitoneally at 1 mg/g, and livers were collected at 30 and 60 minutes and assessed for MET activation as indicated.

findings are the first to show that the HGF-MET axis is blocked in human NASH and provide insight into molecular mechanisms involved in NASH pathogenesis. Lastly, we generated a potent stable agonist of MET (the receptor for HGF), which we have named META4 and used it not only to restore HGF-MET function and to combat NASH in this novel humanized animal model, but to also discover the genes regulated in hepatocytes by the HGF-MET axis.

It has been reported that fatty liver not only causes hepatocyte death (due to lipotoxicity, which promotes oxidative stress and inflammatory cytokine and chemokine induction) but also inhibits hepatocyte proliferation and liver regeneration. Specifically, it was shown that mice with

diet-induced NAFLD exhibit diminished liver regeneration in response to partial hepatectomy.[36] We found that HFD significantly ($P = .002$) represses HGF in wild-type mice and induces HGF antagonist expression. Notably, the HGF-MET axis has been shown to be essential for liver regeneration in experimental models.[21,22] Our results showed that restoring HGF-MET function (by META4 therapy) in a humanized NASH model results in proliferation and expansion of the transplanted human hepatocytes in vivo under toxic insults such as those provoked by lipotoxicity. META4 therapy also completely abrogated inflammation and led to repair of the injured liver. Given the fact that META4 exclusively affects human hepatocytes (because it is specific

Figure 14. Restoration of MET signaling by META4 therapy ameliorates liver inflammation and fibrosis in the humanized NASH and promotes expansion of the transplanted human hepatocytes. *A*, Shown are representative images of liver sections from humanized mice with NASH treated with META4 or with mIgG1 stained for the indicated markers. *B-D*, Confirmation of META4 effects at the protein level. *A*, Alpha smooth muscle actin (α-SMA); *B*, Vimentin; and *C*, IKBa. Livers from nontransplanted (non-TXP) FRGN and ob/ob mice are included for comparison (n = 4) for META4 and (n = 2) for and control.
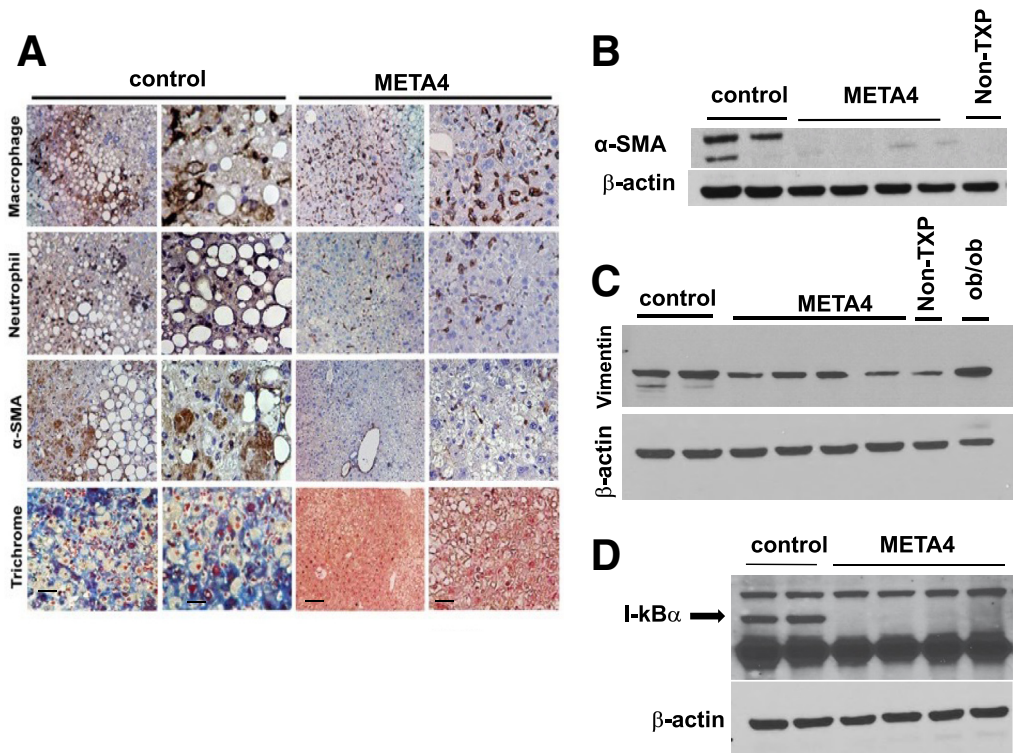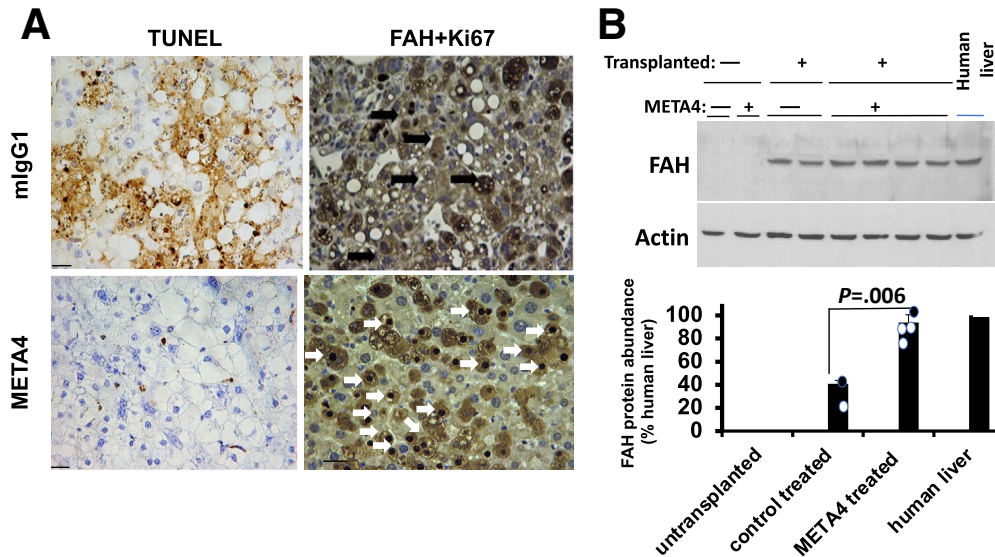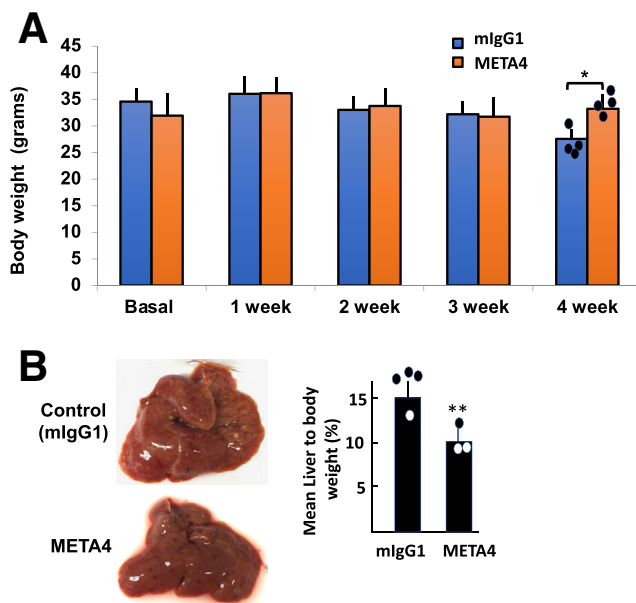
Figure 15. META4 promotes survival and proliferation of human hepatocytes in humanized NASH model. Shown are representative images of liver sections stained for TUNEL (*A*) and Ki67 and FAH double staining as indicated. Scale: 100 mm in the left panel and 30 mm in the right panel, respectively. *Black arrows* point to FAH-positive and Ki67-negative, and *white arrows* point to hepatocytes positive for FAH and nuclear Ki67. Mice were on HFD for 6 weeks and then 4 weeks of META4 therapy (single intraperitoneal injection weekly). *B*, Results of Western blot for FAH indicating expansion (survival and proliferation) of human hepatocytes by META4.

for human MET and does not activate murine MET), the data indicate that the injured hepatocytes are the instigators of liver inflammation and damage by promoting the recruitment of inflammatory cells, for instance.

Figure 16. META4 therapy ameliorates weight lost (*A*) and hepatomegaly (*B*) in mice with humanized liver. *A*, Bar graphs show gradual weight loss in control-treated mice after NTBC withdrawal. *P* = .016. Significance was assessed by the Student *t* test (n = 7 per group). *B*, Shown are the gross appearance of livers and plots of liver to body ratios for META4- (n = 4) or mIgG1(n = 4) treated mice as indicated. **P* = .01.

In the liver, specialized nonparenchymal cells known as hepatic stellate cells mainly express the HGF gene in the liver, and HGF expression becomes repressed in these cells as they undergo activation and de-differentiation into myofibroblastic cells.[37] HGF antagonist isoforms NK1 and NK2 are produced by alternative splicing of the pre-mRNA for HGF, which yields truncated HGF versions that retain part of the N-terminal portion, which is responsible for MET binding but lack kringles 3 and 4 and the entire beta chain of HGF, which are essential for MET dimerization and activation. We found that the ratio of mRNA of HGF to that of HGF antagonists NK1 and NK2 is more than 10 to 1 in normal human liver. In NASH liver as compared with normal liver, the abundance of NK1 and NK2 transcripts increases significantly. We postulate that lipotoxicity alters HGF mRNA splicing resulting in an isoform switch from full length (canonical) HGF to truncated HGF antagonists. Future studies are warranted to decipher the molecular mechanisms involved in upregulation of NK1 and NK2 in the diseased liver setting (such as NASH) and identify the exact cellular origin of these antagonists in the liver (ie, hepatic stellate cells, fatty hepatocytes, Kupffer cells, and other inflammatory cells like neutophils).

Another important finding is that the innate immune cells like macrophages and neutrophils drive hepatic inflammation and injury in our humanized NASH model in the background of fatty human hepatocytes just like that seen in human NASH. Macrophages and neutrophils are well-known to be the major culprits inciting liver injury in human NASH liver contributing to the demise of hepatocytes. There is little or no infiltration of T and B lymphocytes in human NASH as opposed to viral hepatitis and autoimmune hepatitis. In fact,
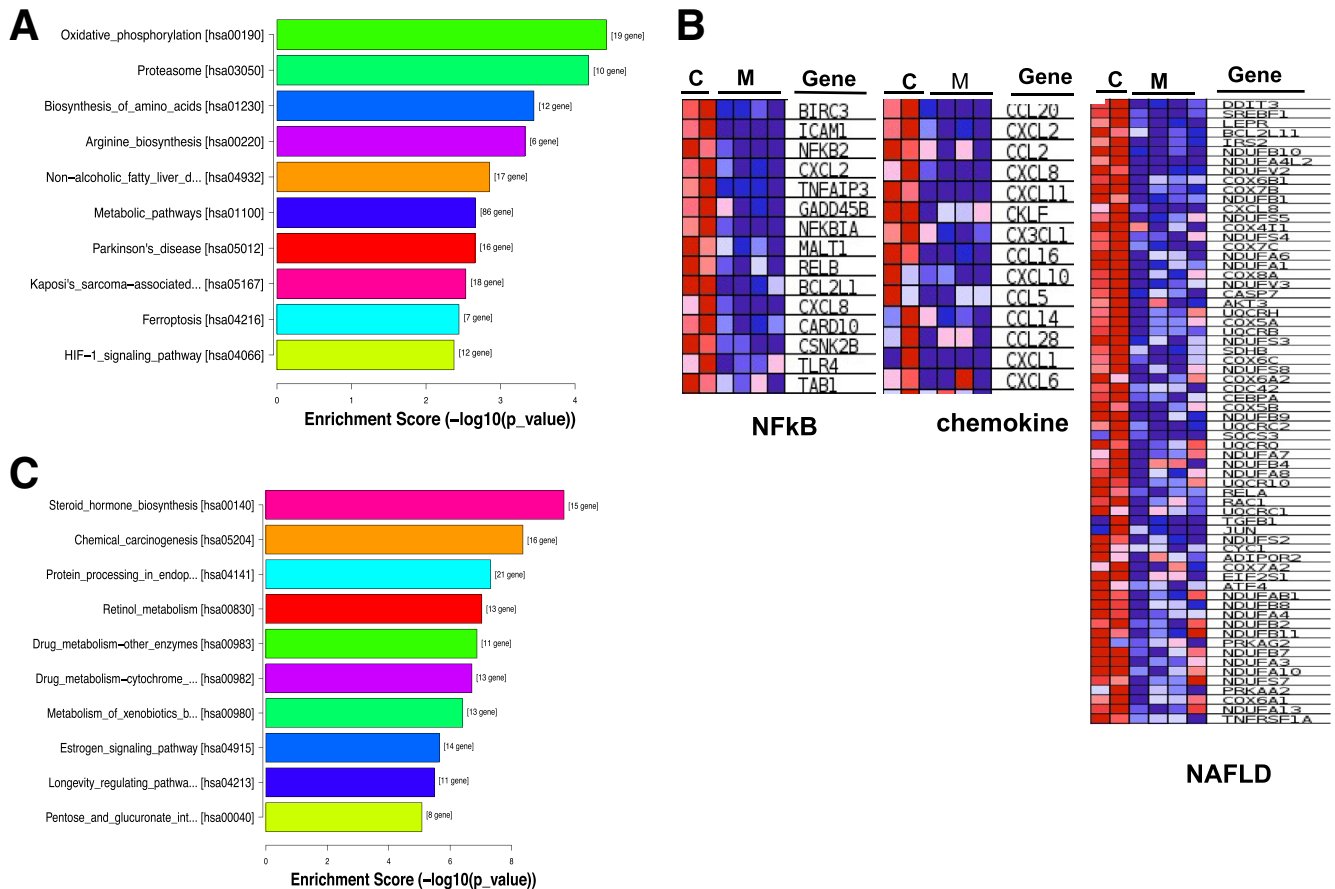
Figure 17. HGF-MET axis promotes down regulation of pathways involved in NAFLD, inflammation, oxidative phosphorylation, and cell death as determined by RNA-seq. Depicts the top 10 pathways that are downregulated (*A*) or upregulated (*B*) by META4 (bar graph colors are arbitrary). Pathway names and number of genes impacted are indicated in the graphs. Pathways are ordered by *P* values from top to bottom. *C*, Illustrates heat maps of the NFkB, chemokine, and NAFLD pathways and their effector genes as determined by gene set enrichment analysis (GSEA). *Red* and *blue* colors indicate induced and repressed genes, respectively. C denotes control and M indicates META4-treated, respectively. A total of 12 humanized mice were analyzed (n = 5 for control and n = 7 for META4 group).

reports show that macrophages play a key role in NASH development in the diet-induced model in wild type mice. The authors demonstrated that elimination of hepatic macrophages by administration of the chemical cladronate diminished the NASH phenotype. And a role for chemokine/chemokine receptor was proposed in macrophage recruitment and accumulation in the liver.[38] Other studies have shown that neutrophil and macrophage infiltration of the liver also plays a critical role in NASH promotion and that depletion of these cell types dampens NASH development.[39,40] We discovered marked macrophage and neutrophil accumulation in our humanized NASH model closely mimicking the phenotype seen in human NASH and diet-induced NASH in murine models. Our data reveal that the culprits inciting liver inflammation in response to lipotoxicity are indeed the fat-laden human hepatocytes, which release monokines/cytokines and chemoattractants to recruit and activate host inflammatory host cells like macrophages and neutrophils. Through transcriptomic (RNA-seq and microarray) studies, we found that a variety of chemokine ligands

and receptors such as CXCL2 and (a potent attractant for polymorphonuclear leukocytes), CCL20 (a neutrophil attractant thought to play an important role in NASH development and progression[38]), and several cytokines/cytokine receptors (like TNFR1, TNFR2, TRAIL, TWEAKR, Fas, and ICAM1) are upregulated in humanized NASH. Notably, we found that META4 therapy repressed the expression of some of these like TWEAKR, RIPK1, and CCL20.

An important corollary revealed by our work is that META4 not only has therapeutic applicability to the treatment of liver diseases in which hepatocytic damage and death prevail (like NASH and other forms of hepatitis) but also likely has therapeutic potential to promote repair of other damaged organs and tissues in which the HGF-MET axis is known to be functionally important. We believe that future studies that assess META4 efficacy for treating degenerative diseases using non-human primate models and humanization of META4 are warranted. Additionally, studies of its safety and potential undesirable side effects (such as fostering tumorigenesis) are also logical. We should

emphasize that we did not detect any evidence of liver tumor development in our humanized mice treated with META4, including no evidence of human hepatocyte dysplasia and no increase in alpha-fetoprotein expression in the liver. In fact, expression of human albumin mRNA in the META4-treated humanized livers was even higher than normal human liver assayed side-by-side in RNA-seq analyses. We believe that the many benefits of restoring the HGF-MET axis by META4 treatment overcome concerns about its potential pro-tumorigenic effect. In fact, activation of the HGF-MET axis may even curtail tumorigenesis by promoting tissue repair and healing, as chronic tissue injury is thought to be a major driver of carcinogenesis. In support of this claim, some studies have shown that HGF offers protective properties against cancer. For example, it was reported that injection of HGF to rats suppresses carcinogen-induced hepatocyte transformation.[41] Using genetic approaches like transgenic mice, others showed that the HGF-MET axis inhibits liver tumorigenesis in these experimental mouse models. Specifically, they reported that hepatocyte-specific elimination of MET in the liver in mice (ie, MET knock out mice) caused enhanced hepatocarcinogenesis,[42] whereas overexpression of HGF in the liver in transgenic mice reduced liver tumorigenesis.[43] Also, various factors that induce growth such as growth hormone, hematopoietic growth factors, and insulin (insulin receptors share close similarity to MET in signal transduction) have been safely administered to patients for decades. Future studies using nonhuman primate models could be helpful to assess the effectiveness and safety profile of META4 therapy in various degenerative models including NASH.

Conclusion

The Figure depicted in the graphical abstract summarizes our proposed model illustrating that lipid accumulation in hepatocytes and lipotoxicity results in dysregulation of cytokine and monokine production and dedifferentiation (activation) of hepatic stellate cells into myofibroblasts. This activation, in turn, changes the process of HGF mRNA alternative splicing event and upregulates NK1/NK2 antagonist isoforms production. Cytokines/monokines may also inhibit HGFAC expression by hepatocytes but also induce expression of protease inhibitor PAI-1, which inhibits HGFAC. The net result is that MET signaling is curtailed and chronic hepatocyte injury leads to fibrosis and NASH. META4 therapy restores MET function and liver homeostasis and ameliorates NASH.

Methods

Generation of Mice With Humanized Liver and High-fat Diet Feeding

The Institutional Care and Use Committee of the University of Pittsburgh approved all mouse experiments. FRGN (*Fah*^{−/−}; *Rag2*^{−/−}; *Interleukin 2 common Gamma chain*^{−/−}; Nod background) were used for generation of mice with humanized livers as described.[8,9] In brief, recipient mice (males and females, 2–3 months old) were transplanted intrasplenically with one million freshly isolated human

hepatocytes obtained from the Liver Tissue Cell Distribution System at the University of Pittsburgh. Human hepatocytes were derived from healthy liver tissue from patients undergoing surgical resection for biliary stricture and hepatolithiasis (gallstones) or benign liver tumor. One donor was a 43-year-old female with biliary stricture and hepatolithiasis, and the other 2 donors had benign liver tumors (a 29-year-old female and a 60-year-old male). None had evidence of fatty liver. All chimeric mice used in our NAFLD experiments had a similar level of human serum albumin of about 3 mg/mL and were used approximately 6 to 8 months post-transplantation. HFD ("Western diet") was obtained from Harlan Laboratory. Mice were fed this diet or regular chow (RD) for a total of 6 to 10 weeks as indicated. Nontransplanted FRGN mice on the same regimen were also used as an additional control. For META4 therapy, mice were placed on HFD and then randomly divided to control (isotype matched mIgG1) or META4 treated groups (7 mice per group). META4 or isotype matched mIgG1 (control) were administered at 1 mg/kg body weight in sterile saline via weekly intraperitoneal injection. To decipher the pro-growth, pro-regenerative activities of META4 on the homeostasis of the transplanted hepatocytes under the lipotoxic conditions, mice placed on the same NTBC regimen consisting of 3 cycles of NTBC withdrawal lasting 2 weeks for each cycle.

Generation of Mice With Humanized Liver and High-fat Diet Feeding

The Institutional Care and Use Committee of the University of Pittsburgh approved all mouse experiments. FRGN (*Fah*^{−/−}; *Rag2*^{−/−}; *Interleukin 2 common Gamma chain*^{−/−}; Nod background) were used for hepatocyte repopulation studies (Yecuris, Inc, Tualatin, OR). FRGN mice were housed in a specific-pathogen free facility and maintained on 8 mg/mL NTBC (Ark Pharm, Libertyville, IL) in the drinking water. Chimeric mice were generated essentially as described.[8,9] In brief, recipient mice (males and females, 2–3 months old) were transplanted intrasplenically with one million freshly isolated human hepatocytes obtained from the Liver Tissue Cell Distribution System at the University of Pittsburgh. Human hepatocytes were derived from healthy liver tissue from patients undergoing surgical resection for biliary stricture and hepatolithiasis (gallstones) or benign liver tumor. One donor was a 43-year-old female with biliary stricture and hepatolithiasis, and the other 2 donors had benign liver tumors (a 29-year-old female and a 60-year-old male). None had evidence of fatty liver. Transplanted mice were maintained on 8 mg/mL NTBC for 4 days following transplantation, and NTBC was then removed to promote expansion of human hepatocytes. Mice were cycled off/on NTBC for 5 to 8 months to achieve a high-level human hepatocyte chimerism. The extent of human hepatocyte chimerism was assessed by measuring human albumin in the blood of repopulated mice (Human Albumin ELISA Quantitation Set, E80-129, Bethyl Laboratories).

All chimeric mice used in our NAFLD experiments had a similar level of human serum albumin of about 3 mg/mL

and were used approximately 6 to 8 months post-transplantation. HFD ("Western diet") was obtained from Harlan Laboratory. Mice were fed this diet or regular chow (RD) for a total of 6 to 10 weeks as indicated. Non-transplanted FRGN mice on the same regimen were also used as an additional control. For META4 therapy, mice were placed on HFD and then randomly divided to control (isotype matched mIgG1) or META4 treated groups (n = 4 per group). META4 or isotype matched mIgG1 (control) were administered at 1 mg/kg body weight in sterile saline via weekly intraperitoneal injection.

Human Liver Samples for Transcriptomic and Proteomic Analyses

Liver specimens were obtained from University of Pittsburgh Health Sciences Tissue Bank according to approved institutional review board protocol. The NASH samples were biopsy-confirmed cases (diagnosed by the Department of Pathology at our institution). Human plasma from normal and biopsy-proven NASH subjects was obtained from Discovery Life Sciences (https://www.dls.com/).

Histology and Immunohistostaining

Assessments of liver damage and hepatocyte death such as TUNEL and fibrosis were performed as described previously.[44,45] Identification of inflammatory cells using macrophage and neutrophil markers was carried out using F4/80 and NIMP-R14 antibodies. Image J was used for quantification of signals. Antibodies against HGF were as follows: N-terminal HGF antibody called Ab1 and Ab2 were from Sigma Aldrich.

RNA-SEQ Analyses

RNA-Seq and bioinformatics analyses were carried out by ArrayStar Inc (arraystar.com). Differentially expressed genes and transcripts analyses were performed using Ballgown R package. Fold change (cutoff 1.5), P-value ($< .05$), and FPKM (>0.5 mean in one group) were used for filtering differentially expressed genes and transcripts. Reads were aligned against human genomic reference (and mouse genomic reference in the case of humanized livers, where indicated in the results). Human NASH and normal livers were 3 cases per group, and humanized NASH and normal livers consisted of 2 to 4 cases per group. In the case of human liver samples, as expected, greater than 95% (mean value n = 6) of the reads were mapped to the human reference. Only approximately 24% (mean value n = 6) of the reads from humanized livers (on HFD or on RD) mapped to the human genomic reference. Conversely, about 75% of the reads from humanized liver mapped to the mouse genomic reference, whereas greater than 95% of the reads from the nontransplanted livers mapped to the mouse genomic reference. These outcomes are anticipated because the humanized liver is composed of mouse parenchymal and nonparenchymal cells plus the transplanted human hepatocytes (see also Discussion).

Microarray Studies

Expression profiling was carried out at the High Throughput Genome Center, UPMC Department of Pathology (http://path.upmc.edu/genome/Index.htm) core using the Affymetrix platform. We used the human Affymetrix U133 Plus 2.0 Array. This array has more than 54,000 probes. We detected about 11,000 probe/genes being expressed in human liver and in humanized liver. All RNA samples were processed and subjected to array analyses side-by-side to minimize variation; livers from 2 different subjects/mice were used. To control for probe specificity, we also used FRGN mouse liver in these experiments. As expected, most probes are specific for human targets and are not conserved in mouse, and we detected about 3800 genes/probes expressed in the mouse liver. Microarray analysis was carried out as we described.[24]

Reverse Transcription Polymerase Chain Reaction Analysis and Sequence Verification for NK1/2

RNA was prepared from human liver tissues using TRIzol (Thermo Fisher, cat# 15596026) according to the manufacturer's instructions. NK1 and NK2 expression were detected by reverse transcription PCR analysis using 5 μg of RNA in 20 μl of reactions comprised of components of Promega GoScript Reverse Transcription System (Fisher Scientific, cat# A5000) according to the instructions provided. Briefly, RNA mixture was denatured at 65°C for 10 minutes and chilled on ice, then the mixture was incubated at 42°C for 1 hour, and reverse transcriptase was inactivated at 70°C for 15 minutes. For amplification, 1 μl of the synthesized cDNA was added to 25 μl of PCR mixture containing Taq DNA Polymerase System (Thermo Fisher, cat#: 10342020). PCR analysis was performed for 40 cycles; β-actin was used as internal control. The forward PCR primer sequence for NK1 is: 5′-GCATCATTGGTAAAGGACGCAGC-3′, and the reverse primer sequence for NK1 is: 5′-GCAT-TAATCTGGTGATAATCCAACAG-3′. The amplified PCR product for NK1 is 508 bp. The forward PCR primer of NK2 is: 5′-CGCTACGAAGTCTGTGACATTCC-3′, and the reverse PCR primer for NK2 is: 5′-CTTCACTGCAGCCTCTGTCACTC-3′. The amplified PCR product for NK2 is 344 bp. The PCR products were analyzed on 2% of agarose gel. The specific DNA bands were cut off from gels and purified using QIAquick Gel Extraction Kit (QIAGEN, cat#: 28704); they were subcloned into PCR 2.1 vector using TA Cloning™ Kit (Thermo Fisher, cat#: K200001). Clones were grown; plasmid DNA was isolated and subjected to DNA sequencing by the University of Pittsburgh Genomic Core facility.

Production and Characterization of META4

Mouse monoclonal antibodies against the extracellular domain of human MET were produced according to standard methods. In brief, mice were immunized with the extracellular domain of purified recombinant human MET (R&D hMET-Fc). Enzyme-linked immunosorbent assay-positive hybridoma clone supernatant purified by protein-

A was assayed in our laboratory for MET activation. Production of the antibody, its cDNA cloning from hybridomas (its heavy and light chains) and generation of META4 expression vectors were all carried out by the vendor Creative Biolabs (www.creative-biolabs.com). Recombinant META4 was also produced in our laboratory by transfecting HEK-293 cells with META4 expression vectors and purified by protein-A chromatography.

Statistics

The 2-tailed Student t test, 1-way analysis of variance, and the Fisher Exact test were used to analyze data as indicated. A P value equal to .05 or less was considered significant in all statistical analyses.

References

1. Younossi ZM, Koenig AB, Abdelatif D, Fazel Y, Henry L, Wymer M. Global epidemiology of nonalcoholic fatty liver disease: meta-analytic assessment of prevalence, incidence, and outcomes. Hepatology 2016;64:73–84.

2. Rinella M, Charlton M. The globalization of nonalcoholic fatty liver disease: prevalence and impact on world health. Hepatology 2016;64:19–22.

3. Anstee QM, Targher G, Day CP. Progression of NAFLD to diabetes mellitus, cardiovascular disease or cirrhosis. Nat Rev Gastroenterol Hepatol 2013;10:330–344.

4. Smith BW, Adams LA. Nonalcoholic fatty liver disease and diabetes mellitus: pathogenesis and treatment. Nat Rev Endocrinol 2011;7:456–465.

5. Hardy T, Oakley F, Anstee QM, Day CP. Nonalcoholic fatty liver disease: pathogenesis and disease spectrum. Annu Rev Pathol 2016;11:451–496.

6. Takahashi Y, Soejima Y, Fukusato T. Animal models of nonalcoholic fatty liver disease/nonalcoholic steatohepatitis. World J Gastroenterol 2012;18:2300–2308.

7. Hebbard L, George J. Animal models of nonalcoholic fatty liver disease. Nat Rev Gastroenterol Hepatol 2011; 8:35–44.

8. Azuma H, Paulk N, Ranade A, Dorrell C, Al-Dhalimy M, Ellis E, Strom S, Kay MA, Finegold M, Grompe M. Robust expansion of human hepatocytes in Fah-/-/Rag2-/-/Il2rg-/- mice. Nat Biotechnol 2007;25:903–910.

9. Wilson EM, Bial J, Tarlow B, Bial G, Jensen B, Greiner DL, Brehm MA, Grompe M. Extensive double humanization of both liver and hematopoiesis in FRGN mice. Stem Cell Res 2014;13(3 Pt A):404–412.

10. Strom SC, Davila J, Grompe M. Chimeric mice with humanized liver: tools for the study of drug metabolism, excretion, and toxicity. Methods Mol Biol 2010; 640:491–509.

11. Grompe M, Strom S. Mice with human livers. Gastroenterology 2013;145:1209–1214.

12. Velazquez KT, Enos RT, Bader JE, Sougiannis AT, Carson MS, Chatzistamou I, Carson JA, Nagarkatti PS, Nagarkatti M, Murphy EA. Prolonged high-fat-diet feeding promotes non-alcoholic fatty liver disease and alters gut microbiota in mice. World J Hepatol 2019; 11:619–637.

13. Johnson JM, Castle J, Garrett-Engele P, Kan Z, Loerch PM, Armour CD, Santos R, Schadt EE, Stoughton R, Shoemaker DD. Genome-wide survey of human alternative pre-mRNA splicing with exon junction microarrays. Science 2003;302:2141–2144.

14. Chan AM, Rubin JS, Bottaro DP, Hirschfield DW, Chedid M, Aaronson SA. Identification of a competitive HGF antagonist encoded by an alternative transcript. Science 1991;254:1382–1385.

15. Miyazawa K, Kitamura A, Naka D, Kitamura N. An alternatively processed mRNA generated from human hepatocyte growth factor gene. Eur J Biochem 1991; 197:15–22.

16. Lokker NA, Mark MR, Luis EA, Bennett GL, Robbins KA, Baker JB, Godowski PJ. Structure-function analysis of hepatocyte growth factor: identification of variants that lack mitogenic activity yet retain high affinity receptor binding. EMBO J 1992;11:2503–2510.

17. Mars WM, Zarnegar R, Michalopoulos GK. Activation of hepatocyte growth factor by the plasminogen activators uPA and tPA. Am J Pathol 1993;143:949–958.

18. Thuy S, Ladurner R, Volynets V, Wagner S, Strahl S, Konigsrainer A, Maier KP, Bischoff SC, Bergheim I. Nonalcoholic fatty liver disease in humans is associated with increased plasma endotoxin and plasminogen activator inhibitor 1 concentrations and with fructose intake. J Nutr 2008;138:1452–1455.

19. Chang ML, Hsu CM, Tseng JH, Tsou YK, Chen SC, Shiau SS, Yeh CT, Chiu CT. Plasminogen activator inhibitor-1 is independently associated with non-alcoholic fatty liver disease whereas leptin and adiponectin vary between genders. J Gastroenterol Hepatol 2015;30:329–336.

20. Arteel GE. New role of plasminogen activator inhibitor-1 in alcohol-induced liver injury. J Gastroenterol Hepatol 2008;23(Suppl 1):S54–S59.

21. Huh CG, Factor VM, Sanchez A, Uchida K, Conner EA, Thorgeirsson SS. Hepatocyte growth factor/c-met signaling pathway is required for efficient liver regeneration and repair. Proc Natl Acad Sci U S A 2004;101: 4477–4482.

22. Borowiak M, Garratt AN, Wustefeld T, Strehle M, Trautwein C, Birchmeier C. Met provides essential signals for liver regeneration. Proc Natl Acad Sci U S A 2004;101:10608–10613.

23. Michalopoulos GK, DeFrances MC. Liver regeneration. Science 1997;276:60–66.

24. Fafalios A, Ma J, Tan X, Stoops J, Luo J, Defrances MC, Zarnegar R. A hepatocyte growth factor receptor (Met)-insulin receptor hybrid governs hepatic glucose metabolism. Nat Med 2011;17:1577–1584.

25. Nakamura T, Mizuno S. The discovery of hepatocyte growth factor (HGF) and its significance for cell biology, life sciences and clinical medicine. Proc Jpn Acad Ser B Phys Biol Sci 2010;86:588–610.

26. Kiyama S, Yamada T, Iwata H, Sekino T, Matsuo H, Yoshida N, Miyahara T, Umeda Y, Matsuno Y, Kimura M, Matsumoto K, Nakamura T, Takemura H. Reduction of fibrosis in a rat model of non-alcoholic steatohepatitis cirrhosis by human HGF gene transfection using

electroporation. J Gastroenterol Hepatol 2008;23(8 Pt 2): e471–e476.

27. Ozawa S, Uchiyama K, Nakamori M, Ueda K, Iwahashi M, Ueno H, Muragaki Y, Ooshima A, Yamaue H. Combination gene therapy of HGF and truncated type II TGF-beta receptor for rat liver cirrhosis after partial hepatectomy. Surgery 2006;139:563–573.

28. Kessler JA, Smith AG, Cha BS, Choi SH, Wymer J, Shaibani A, Ajroud-Driss S, Vinik A. VM202 DPN-II Study Group. Double-blind, placebo-controlled study of HGF gene therapy in diabetic neuropathy. Ann Clin Transl Neurol 2015;2:465–478.

29. Jin H, Wyss JM, Yang R, Schwall R. The therapeutic potential of hepatocyte growth factor for myocardial infarction and heart failure. Curr Pharm Des 2004; 10:2525–2533.

30. Ido A, Moriuchi A, Marusawa H, Ikeda K, Numata M, Yamaji N, Setoyama H, Ida H, Oketani M, Chiba T, Tsubouchi H. Translational research on HGF: a phase I/II study of recombinant human HGF for the treatment of fulminant hepatic failure. Hepatol Res 2008;38(Suppl 1): S88–S92.

31. Appasamy R, Tanabe M, Murase N, Zarnegar R, Venkataramanan R, Van Thiel DH, Michalopoulos GK. Hepatocyte growth factor, blood clearance, organ uptake, and biliary excretion in normal and partially hepatectomized rats. Lab Invest 1993; 68:270–276.

32. Gohda E, Tsubouchi H, Nakayama H, Hirono S, Sakiyama O, Takahashi K, Miyazaki H, Hashimoto S, Daikuhara Y. Purification and partial characterization of hepatocyte growth factor from plasma of a patient with fulminant hepatic failure. J Clin Invest 1988; 81:414–419.

33. Shimizu I, Ichihara A, Nakamura T. Hepatocyte growth factor in ascites from patients with cirrhosis. J Biochem 1991;109:14–18.

34. Wu AL, Kolumam G, Stawicki S, Chen Y, Li J, Zavala-Solorio J, Phamluong K, Feng B, Li L, Marsters S, Kates L, van Bruggen N, Leabman M, Wong A, West D, Stern H, Luis E, Kim HS, Yansura D, Peterson AS, Filvaroff E, Wu Y, Sonoda J. Amelioration of type 2 diabetes by antibody-mediated activation of fibroblast growth factor receptor 1. Sci Transl Med 2011;3: 113ra126.

35. Foltz IN, Hu S, King C, Wu X, Yang C, Wang W, Weiszmann J, Stevens J, Chen JS, Nuanmanee N, Gupte J, Komorowski R, Sekirov L, Hager T, Arora T, Ge H, Baribault H, Wang F, Sheng J, Karow M, Wang M, Luo Y, McKeehan W, Wang Z, Veniant MM, Li Y. Treating diabetes and obesity with an FGF21-mimetic antibody activating the betaKlotho/FGFR1c receptor complex. Sci Transl Med 2012;4:162ra153.

36. DeAngelis RA, Markiewski MM, Taub R, Lambris JD. A high-fat diet impairs liver regeneration in C57BL/6 mice through overexpression of the NF-kappaB inhibitor, IkappaBalpha. Hepatology 2005;42:1148–1157.

37. Schirmacher P, Geerts A, Pietrangelo A, Dienes HP, Rogler CE. Hepatocyte growth factor/hepatopoietin A is expressed in fat-storing cells from rat liver but not myofibroblast-like cells derived from fat-storing cells. Hepatology 1992;15:5–11.

38. Marra F, Tacke F. Roles for chemokines in liver disease. Gastroenterology 2014;147:577–594 e1.

39. Reid DT, Reyes JL, McDonald BA, Vo T, Reimer RA, Eksteen B. Kupffer cells undergo fundamental changes during the development of experimental NASH and are critical in initiating liver damage and inflammation. PLoS One 2016;11:e0159524.

40. Zang S, Wang L, Ma X, Zhu G, Zhuang Z, Xun Y, Zhao F, Yang W, Liu J, Luo Y, Liu Y, Ye D, Shi J. Neutrophils play a crucial role in the early stage of nonalcoholic steato-hepatitis via neutrophil elastase in mice. Cell Biochem Biophys 2015;73:479–487.

41. Liu ML, Mars WM, Michalopoulos GK. Hepatocyte growth factor inhibits cell proliferation in vivo of rat hepatocellular carcinomas induced by diethylnitrosamine. Carcinogenesis 1995;16:841–843.

42. Takami T, Kaposi-Novak P, Uchida K, Gomez-Quiroz LE, Conner EA, Factor VM, Thorgeirsson SS. Loss of hepatocyte growth factor/c-Met signaling pathway accelerates early stages of N-nitrosodiethyl-amine induced hepatocarcinogenesis. Cancer Res 2007;67:9844–9851.

43. Santoni-Rugiu E, Preisegger KH, Kiss A, Audolfsson T, Shiota G, Schmidt EV, Thorgeirsson SS. Inhibition of neoplastic development in the liver by hepatocyte growth factor in a transgenic mouse model. Proc Natl Acad Sci U S A 1996;93:9577–9582.

Correspondence
Address correspondence to: Prof Reza Zarnegar, University of Pittsburgh, Department of Pathology, 200 Lothrop St, Pittsburgh, Pennsylvania 15261. E-mail: rezazar@pitt.edu; tel: (412) 648-8657; fax: (412) 648-1916.